*"Tribological Applications"*, A. Rodrigo (ed.) © CNEA , Buenos Aires, Argentina (2000) 9–19

# **F**unctional **G**radient **M**aterials (FGM)- New trends in Vacuum Arc Deposition Plasma technology

J. A. Vivas Hohl[*], J.L. Garcia[*,°]. N. V. Vershinin[+], B. B. Straumal[+]

* Master on Technological Materials Science – Facultad de Ingeniería Universidad Nacional del Comahue, Buenos Aires 1400, 8300 Neuquén, Argentina

+ SONG S.L., P.O. Box 98, 142432 Chernogolovka, Moscow District, Russia and I.V.T. S.L. (Institute for Vacuum Technology), P.O. Box 47, 109180 Moscow, Russia

° Institute for Chemical Technology of Inorganic Materials, Vienna University of Technology, Getreidemarkt 9/161, A-1060 Vienna, Austria.

## Abstract

FGM play a relevant role with some impact in coatings industry, a case study is analysed and alternative path on coatings technology through vacuum arc deposition (VAD) routes is presented. The vacuum arc discharges in the vapour of the cathode material are described. In case that several cathodes are used, the possibility exists to control each discharge independently from the others because no reactive gas is needed which can lead to interaction among the discharges of individual cathodes. The deposition rate of each component can be changed during the deposition process *in situ*. It permits to produce gradient coatings. In this work, Ti and Ni were deposited onto silicate glass substrates in a chamber having two separated vacuum arc sources. The discharge power *P* for both cathodes was gradually changed during the deposition process. Depth-profiling of the produced coatings was made with the aid of secondary ion mass spectroscopy. The concentration of Ni is maximal close to the substrate and gradually decreases towards the surface of the coating. The concentration of Ti is least at the substrate and maximal on the surface. The slope of the concentration profiles depends on the distance *L* between the substrate and cathodes. The concentration gradient can be controlled both by changing *P* and *L*.

Keywords: FGM; FGHM; Gradient coatings; Vacuum arc deposition; Deposition rate; Ni; Ti.

## 1. Introduction

In the last years, the role of functional gradient materials (FGM) have been very important in processes and applications. However, in the history is possible to found ancient examples, Figure 1 shows a samurai sword microstructure, that was forged by a earlier medieval Japanese technique, that presented a gradient microstructure and therefore gradient properties, which make such technology very effective at those times. Due to these properties such kind of materials present unquestionable advantages compared with the properties of conventional coatings obtained through physical (PVD), and chemical vapour deposition (CVD) or other deposition routes. A nice example are the cermets and (Ti,W)-C-kind hard metals, which constitute the bases of the materials for the cutting tools. The conventional basic method of their manufacturing includes two stages: first, the sintering of green as far as liquid-fase temperatures (ca. 400ºC) and second, the recovering of the metals by a TiN, TiC or multilayer coating obtained by means of a CVD or PVD process. Thus, the wished final properties of the cutting tool are obtained: a ductile and strong body and a low roughness and high hardness surface [1, 2].

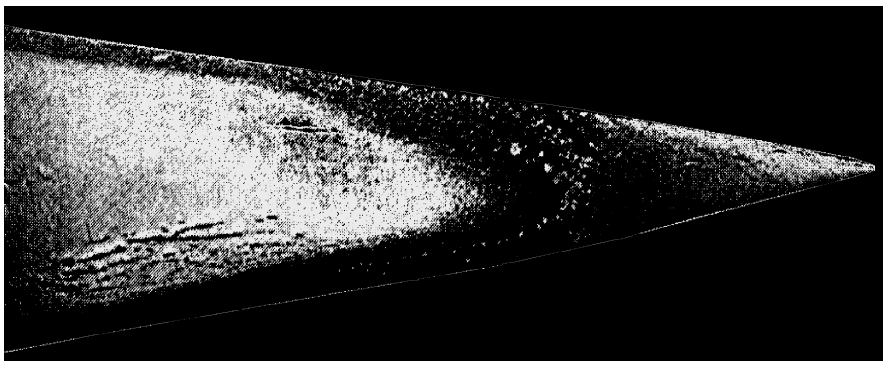

Japanese Samurai Sword - Cross Section (Smith 1960) > 1000 years old

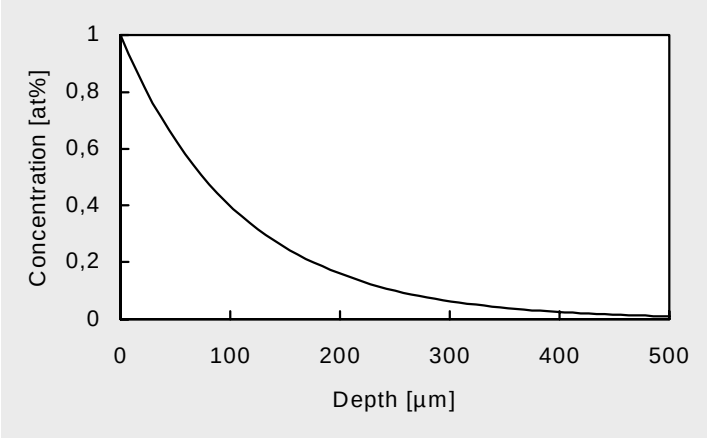


Concentration Profile

Figure 1: Japanese samurai sword and concentration profile

WIDIA-Vanelite produce (Ti,W)-C kind alloys under controlled reactive atmosphere to modify the surface and obtain functional gradient microstructures in only one step. By means of this new process Ti($C_x$,$N_y$) or WC layers are obtained without using plasma deposition methods such us CVD or PVD. This saves a 15-20% of the total cost of the tool manufacturing. Besides, the modified zone and the gradient are homogeneous and they form only one part, avoiding in that way the common recovering process problems such as shallow layer detaching and concentration between the recovering and the substrate. These stresses produce failures in the tools during machining and shorten their life-time. The roughness is similar to the one obtained by means of coating techniques. The hardness and porosity is the same as in the conventional hard materials, and the residual tensions in the Ti(C,N) are zero or those of compression. The microstructure can be controlled by sintering conditions and composition, Figures 2 and 3 [3].

By means of a sintering with controlled atmosphere (controlled diffusion) and adequate compositions, we obtain a functional material with a Ti(C,N) or/and WC modified surface and a gradual and homogeneous distribution of its components. This produces the necessary "functional properties" for the cutting tools: adequate superficial hardness and strength in the rest of their components, Figure 3. This example shows coatings technology would be replaced by the above described treatment, unless it will be possible to produce gradient coatings.

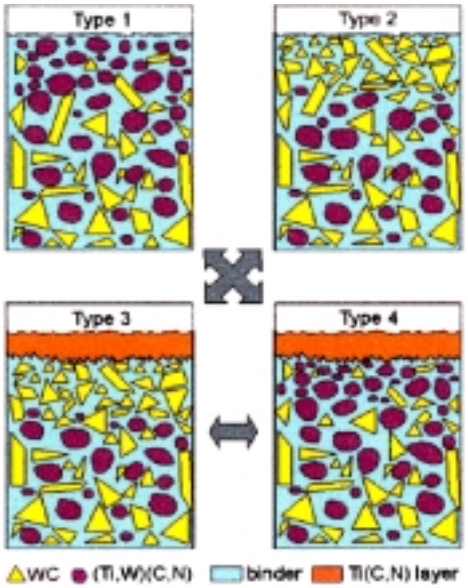


Type 1: a Ti(C,N)-rich surface gradually changes into a structure composed of WC and Ti(C,N)

Type 2: a WC-Co layer onto a graded structure.

Type 3: a Ti(C,N) layer onto a WC-Co zone and a gradient structure like type 2.

Type 4: a Ti(C,N) layer onto a graded structure like type 1.

Fig.2: Scheme of the microstructure of the four principle types of functional-gradient cemented carbonitrides described in [1]. Gradual changes of some types in another are possible (arrows).

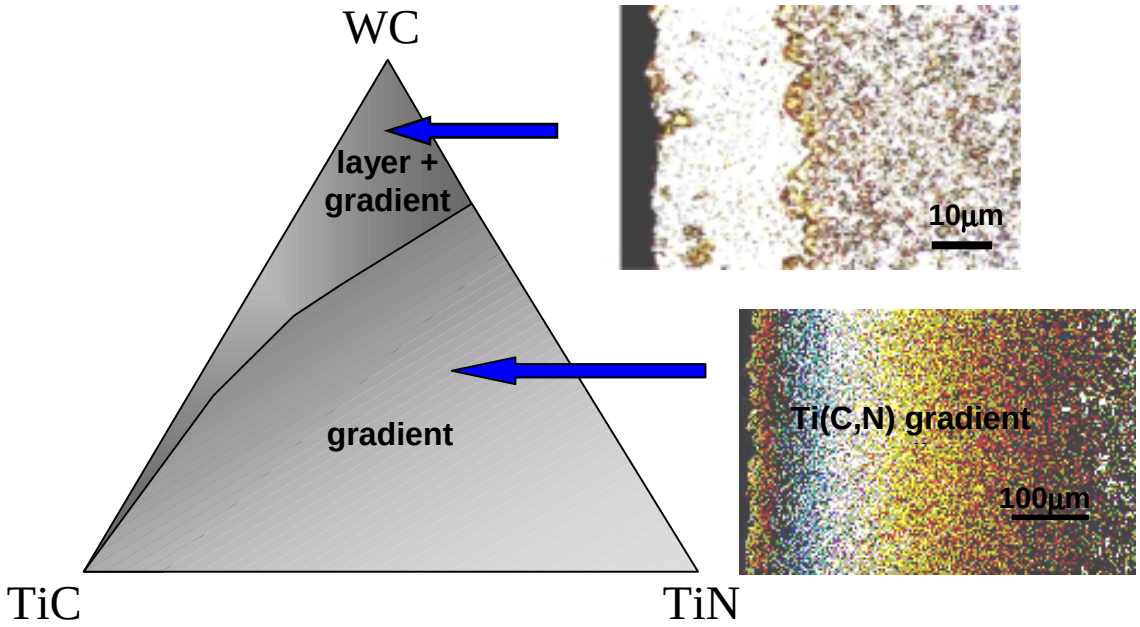


Fig. 3: Main functional-gradient microstructural regions in the WC-TiN-TiC phase diagram.

## 2. Vacuum Arc Deposition of Functionally Gradient Coatings

Functionally gradient coatings form a new class of structures in which the microstructure and properties gradually vary from the surface to the interior of the material. In a number of applications, including the use of coatings for thermal, wear or corrosion resistance, joining of

structural components, and microelectronics, the mismatch in properties at the interface between a coating and a substrate can cause stress concentrations to develop during fabrication or while in service that result in failure of the interface. Functionally gradient coatings offer a potential solution to this problem [4]. The possibility to produce the coatings where the composition gradually changes from the substrate to surface of film can be useful also in many other applications like coatings of turbine blades [5], simultaneous protection against various corrosive media [6], biomaterials for implants [7] and for the substitution of multilayers. For example, the optical films with a gradually varying refractive index in the direction of the normal to the film surfaces have appeared particularly of interest. The almost total absence of reflections from a gradual transition between two media with different indices is promising to develop unusual properties that cannot be realised by stacks of homogenous films [8]. Therefore, the development of the reliable technologies for the controllable deposition of gradient coatings is very important. Recently, the plasma spraying [7], co-evaporation [9, 10], metalorganic spin-coating [11] and jet vapour deposition [12] were used for the production of gradient coatings. The goal of this work is to demonstrate the possibility to produce the gradient coatings with the aid of a vacuum arc deposition. Vacuum arc deposition combines the advantages of the evaporation and sputtering techniques [13]. Vacuum arc discharges in the vapour of the cathode material. It makes possible the simultaneous usage of several sources because no reactive gas is needed which can lead to interaction among the discharges of individual cathodes. This feature permits an easy fabrication of the multicomponent coatings. In case that several cathodes are used, the possibility exists to control each discharge independently of the others. Furthermore, the deposition rate of each component can be changed during the deposition process *in situ*. It permits to produce gradient coatings. The vacuum arc deposition is also suitable for coating three-dimensional parts having complex form.

## 3. Kaufman Source and Hall Current Acelerator

Ion beam processing is an established method for surface treatment [14]. It includes techniques like sputtering, thin film deposition and ion implantation. Though the principle is the same in all cases, a given application requires a specific source design according to the ion energy range and uniformity needed. By the coating of large substrates like glass sheets or steel strips for architectural and structural applications, the substrate cleaning before coating is of particular importance for the adhesion and corrosion resistance of the further deposited layers and, therefore, for the long-term stability of properties and of the appearance of coated parts in various environments. Ion beam sputter precleaning proved to be an efficient method to ensure high quality coating on glass, metal and plastic sheets. For sputtering purposes, Kaufman sources [15-17] are usually chosen. The sources are very attractive in the sense that neutralized beam is generated with independently controllable ion energy and current density. The ion production is also separated from the substrate and target used. However, inherent design considerations limit the use of such sources in production applications [18]. The source cathode and grid optics are critical components which sometimes require excessive maintenance. Local heating or presence of reactive gases (such as oxygen) dramatically reduce the source lifetime by damaging the cathode. Depending on the cathode type, the source lifetime ranges from a few hundred to one thousand hours. Grid optics of Kaufman sources limit the ion beam current that can be extracted from the chamber. In architectural and structural applications the source design must also meet the requirement of a large area treatment.

Large aperture Hall current accelerator was developed for sputter cleaning of a large area glass, metal and plastic sheets. Though less controllable than Kaufman sources, a Hall current accelerator appears better suited for sputter cleaning production requirements [17]. Of greater significance is the lack of any space charge flow limitation on the ion current density. Furthermore, the reliability in etching is improved through the absence of any delicate structures like cathode or grid optics The Hall current accelerator requires little maintenance, and the sputter cleaning can be performed with reactive gases such as oxygen, nitrogen and carbon dioxide. The Hall current accelerator requires little maintenance, and the sputter cleaning can be performed with reactive gases such as oxygen, nitrogen, and carbon dioxide. The scheme of the Hall current accelerator is shown in Figure 4. It has the shape of a very elongated loop. The large aperture (1400 mm in the vertical direction) allow one to use it in the multipurpose apparatus for deposition on large area glass and plastic sheets by vacuum arc deposition [19-21] and magnetron sputtering. Sheets to be treated are successively transported under the Hall discharge accelerator at a given translation speed, substrate surface being perpendicular to the ionic flux axis. The aperture of the Hall current accelerator at a given translation speed, the substrate surface being perpendicular to the ionic flux axis. Changing the speed and accelerator power, one can control the sputter dose received by the substrate. The aperture of the Hall current accelerator can be scaled up to 3000 mm without significant changes in design and, therefore, adjusted to a deposition apparatus. A twin aperture has two slots, 55 mm away from one another. Two juxtaposed permanent magnets act as cathode. The water cooled anode of tubular shape runs inside the groove made by the cathode. The whole apparatus is set under vacuum in the presence of a sputter gas (usually argon). Gas ionization and the subsequent ion acceleration is made through the presence of crossed electric and magnetic fields. The electric field is created by the cathode-to-anode potential drop whereas a quasi-uniform magnetic field is set between the two pole pieces of the cathode. In the presence of a low pressure gas and electric field, a glow discharge plasma is initiated. The magnetic field traps the plasma electrons and, together with the electric field, causes them to precede circumferentially along the anode surface. Through their cycloid path, they collide with argon atoms and ionize them. The high difference of potential accelerates the argon ions away from the anode and towards the substrate to be sputter cleaned [22].

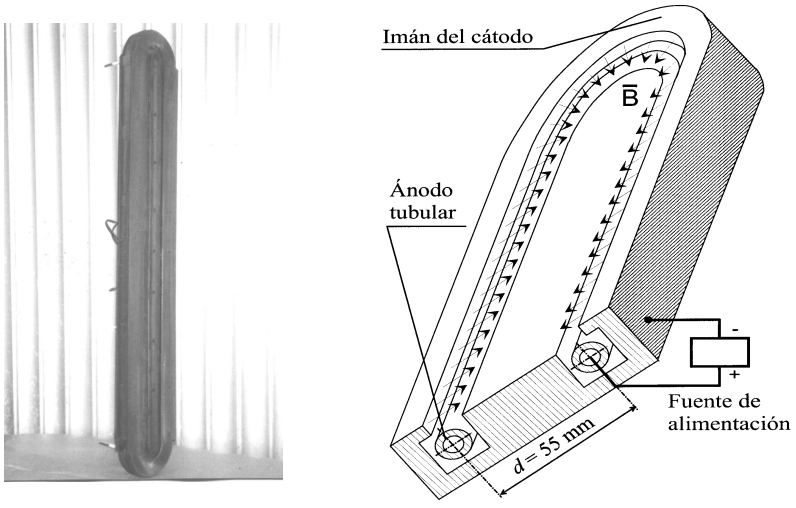


Fig. 4: Hall current accelerator (section through the middle plane). Total length 700 mm

## 4. Case Study – FGM with Ni and Ti Coatings

The vacuum arc device used in this work consists of vacuum chamber having the form of a horizontal cylinder of 700 mm diameter and 700 mm length [23]. Its pumping system consists of a Balzers turbomolecular pump with a capacity of 1500 *l* /s and two rotary pumps with a total capacity of 40 *l* /s. A total pressure of $6\times 10^{-5}$ Pa may be achieved without deposition process. The pressure during deposition is $8\times10^{-4}$ Pa. On opposite ends of the vacuum chamber two vacuum arc sources are placed. Each source possesses the system for spot stabilisation. In this work the Ni cathode was mounted in one source and the Ti cathode was mounted in the second source. Both cathodes have the diameter $D$ = 60 mm. They were made of Ti of 99.98% and Ni of 99.93% purity. The facilities for magnetic filtering of the macroparticles were not used in this work. The material of the anode was not consumed in the arc process. The substrates made from polished silica glass with dimensions of $20\times 20$ mm$^2$ were placed between the Ni and Ti cathodes on various distances $L$ from the surface of the Ni cathode.

The vacuum arc source voltage was maintained constant $U$ = 20 V for Ti and 18 V for Ni. The discharge power $P$ was changed during the deposition independently by changing the discharge current $I_d$ (Ni) and $I_d$ (Ti) of the two sources. $I_d$ (Ni) decreased stepwise from 150 to 80 A while $I_d$ (Ti) increased stepwise from 150 to 300 A (Table 1). Below $I_d$ (Ti) = 150 A and $I_d$ (Ni) = 80 A, the vacuum arc discharge becomes unstable. The strength of the stabilizing magnetic field on the Ti cathode surface was 60 to 70 G. No bias was applied to the substrates. The coating time $t$ was the same for all samples at $t$ = 260 s.

The distribution of Ni and Ti in the coatings was determined using secondary ion mass spectroscopy (SIMS). Secondary ion mass spectrometer *ims 3f* (Cameca, France) has been used for in-depth analyses of the films. Oxygen $O_2^+$ ions accelerated with energy 12.5 kV were used as primary ions. The primary ion current $I_p$ ranged from 400 to 1000 nA. The primary ion beam was rastered over a square area $250 \times 250$ μm. The secondary ions, accelerated by 4.5 kV, were collected from a square area $50\times50$ μm in the middle of the rastered area. The energy band pass filter for the secondary ions was 50 eV, centered at the maximum energy of the secondary ions. The distributions of Ti and Ni were studied by profiling isotopes $Ti_{50}$ and $Ni_{62}$, respectively. The quantification of the secondary ions has been done by analysing coatings of pure titanium and nickel, deposited and analysed under the same conditions as the Ti–Ni gradient coatings. The depths of the sputtered craters were measured with a *Talysurf 10* instrument (Rank Taylor Hobson, England). Each crater has been measured several times in the central region of the crater. The deviation in the average depth ranged from 2 to 11%.

## 5. Results and Discussion

Figure 5 displays the dependence of deposition rate $R_d$ and the coating thickness $d$ on the position of the sample between the Ni and Ti cathodes. $R_d$ and $d$ are maximal close to the Ni and Ti cathodes and decrease with increasing distance from both cathodes. $R_d$ and $d$ reach a minimum at $L$ about 300 mm (from the Ni cathode). $R_d$ and $d$ are about two times higher close to the Ti cathode than close to the Ni cathode due to the higher deposition rate of Ti at the same discharge current $I_d$. Therefore, the minimum of $d(L)$ and $R_d$ $(L)$ is shifted from the middle of a chamber towards the Ni cathode. At comparable $L/D$ ratio and discharge power $P$ ($L/D$ = 0.4, $D$ being the

diameter of the cathode, $P$ = 3 kW), the $R_d$ for Ti is about 2 to 4 times higher than $R_d$ for magnetron sputter deposition [24, 25]. Recently it was shown that $R_d$ for vacuum arc deposition of Mo decreases with increasing $L$ much slower than in case of the magnetron sputter deposition. $R_d$ for Ti decreases with increasing $L$ from the Ti cathode at roughly the same rate as in case of the magnetron sputter deposition, and with increasing $L$ from Ni cathode about 3 to 4 times slower [24]. Therefore, the vacuum arc deposition is generally better suited for the coating of three-dimensional parts having a complex form, in comparison with the magnetron sputter deposition.

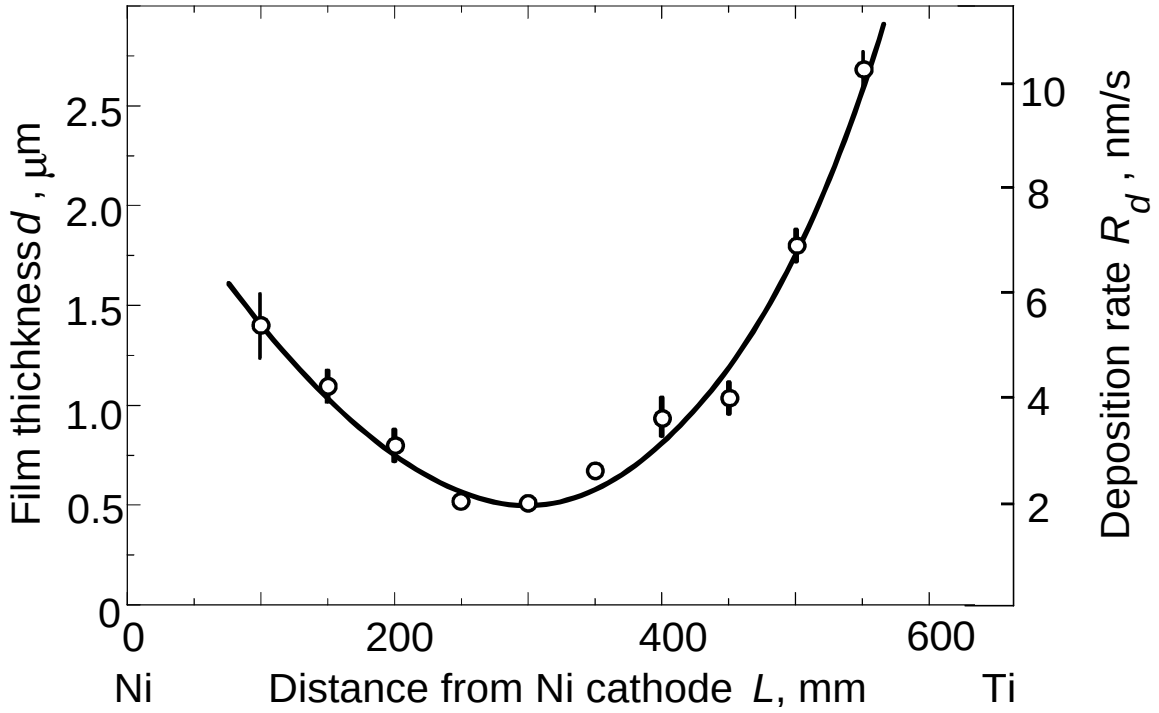


Fig. 5: Dependence of the deposition rate $R_d$ and film thickness $d$ on the position of the sample between the Ni and Ti cathodes.

Table 1.Variation of discharge current $I_d$ for Ti and Ni cathodes in dependence on the deposition time $t_d$.

| $t$, s | 20 | 40 | 60 | 80 | 100 | 120 | 140 | 160 | 180 | 200 | 220 | 240 | 260 |
|---|---|---|---|---|---|---|---|---|---|---|---|---|---|
| $I_d$ (Ni), A | 150 | 150 | 150 | 150 | 150 | 150 | 150 | 140 | 130 | 110 | 100 | 90 | 80 |
| $I_d$ (Ti), A | 150 | 150 | 170 | 200 | 240 | 260 | 300 | 300 | 300 | 300 | 300 | 300 | 300 |

In the Figure 6 the depth profiles of Ni–Ti coatings are displayed for the various distances *L*. The discharge current $I_d$ (Ti) increased and $I_d$ (Ni) decreased gradually during the deposition (s. Table 1). In all samples the concentration of Ti increases from

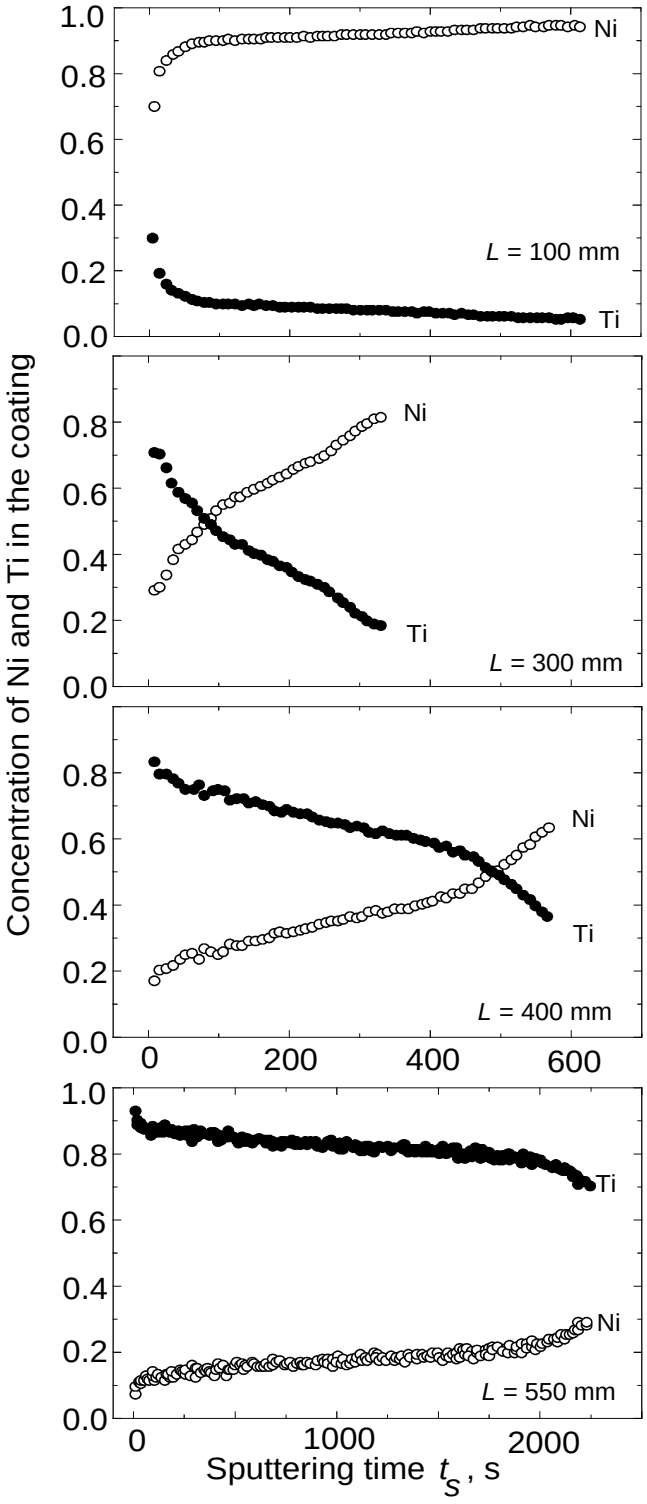


Fig. 6. Depth profiles of Ni–Ti coatings for various distances *L*.

the substrate towards the surface of a coating, and the Ni concentration decreases, conversely. Therefore, by changing $I_d$ during the deposition, one can really control the composition of a coating and reach a gradual change of the concentration. Close to the Ni cathode ($L$ = 100 mm), the coating consists nearly of pure Ni. Only its top part contains an essential amount of Ti. Close to the Ti cathode ($L$ = 550 mm) titanium dominates in the coating. In the middle of a vacuum chamber ($L$ = 300 and 400 mm), the depth profiles of Ti and Ni intersect. The top part of these coatings consist mainly of Ti, and the bottom part mainly of Ni. The intersection point where the concentrations of Ti and Ni are equal moves from the surface of a coating towards the substrate with increasing $L$. The concentration steps originated due to the stepwise change of discharge current, can be clearly seen in the profiles for $L$ = 300 mm. The microdroplets of Ti and Ni are present in the coatings, because the filtering facilities were not used in this work. Neveretheless, the presence of the droplets does not disturb the concentration gradient in the Ni–Ti films.

Figure 7 displays the concentration of Ni and Ti in the coating close to the substrate for various $L$. Both curves intersect at $L$ = 470 mm, rather close to the Ti cathode. At the beginning of a deposition procedure, $I_d$ (Ni) = $I_d$ (Ti) = 150 A. Therefore, the asymmetry of the concentration curves in Fig. 7 clearly demonstrates that the deposition rate for Ni decreases with increasing distance from the cathode slower than $R_d$ for Ti.

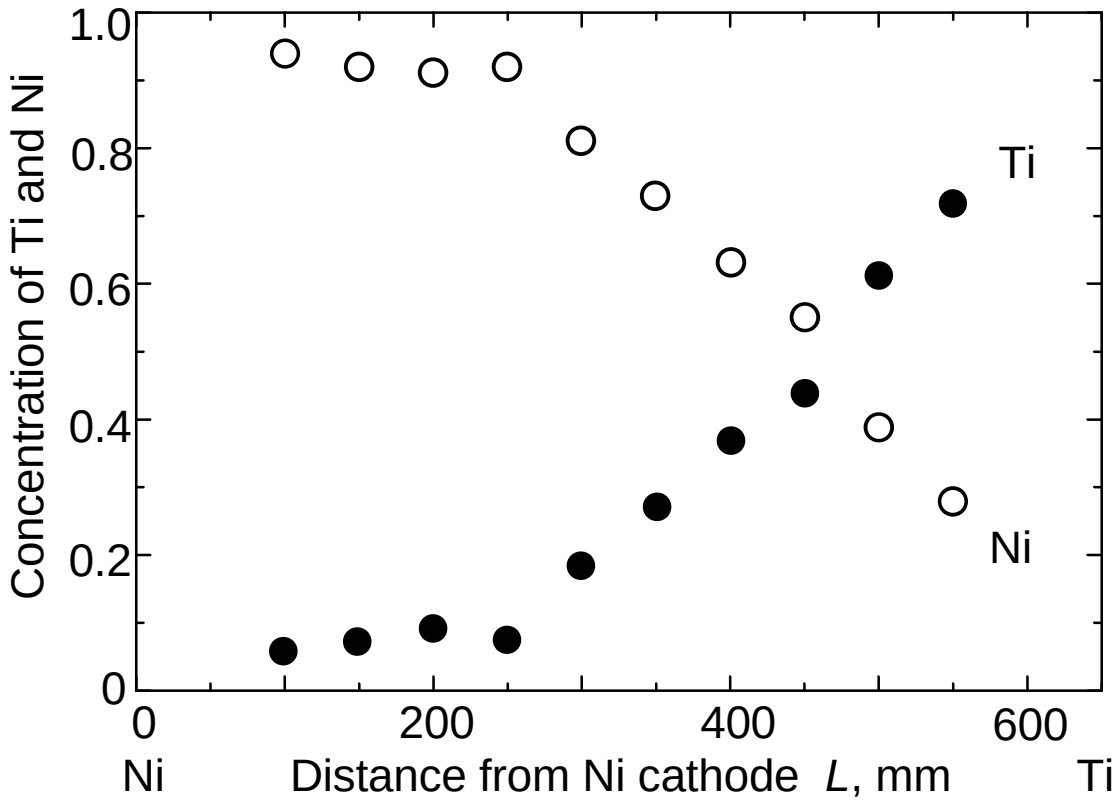


Fig. 7. Dependence of concentration of Ni and Ti in the gradient coatings close to the substrate on the distance $L$.

## 6. Conclusions

- By changing the discharge power of two independent vacuum arc sources with Ti and Ni cathodes during the deposition process, the deposition rate of each component was changed *in situ*.
- As a result, a gradual change of the Ni and Ti concentration in a coating was achieved.
- High deposition rates $R_d$ (Ti) = 10.5 nm/s and $R_d$ (Ni) = 5.5 nm/s are achieved close to the Ni and Ti cathodes.
- The concentration gradient depends on the distance from both cathodes.
- It is possible to control the concentration gradient in a coating *in situ* during the vacuum arc deposition by changing the discharge power and by varying the geometry of the deposition chamber.

## 7. Acknowledgements

The financial support of the **FOMEC** (Fondo para el mejoramiento de la Enseñanza Superior) Proyecto N° 505 of the National Education Ministery, Argentina, **ALFA Proramme** of the **EC,** Network **EDUMAT (Edu**cation on **Mat**erials Science-Contract 98: 6.0256.0), and the Copernicus Network (contract **ERB** IC15 0815), as well as WIDIA-Vanelite co-operation contracts is heartily acknowledged. This work have been carried out through the co-operation of several Universities and research Centres world-wide, Dr. Boris STRAUMAL, Dr. Nikolai VERSHININ, Dipl. Ing. Jose Luis GARCIA and co-workers were involved in different projects and carried out partial results of this paper.

## 8. References

[1] W. Lengauer, L. Chen, J. Garcia, V. Ucakar, K. Dreyer, D. Kassel, H.W. Daub, *Diffusion-Controlled Surface Modification for Fabrication of Functional-Gradient (Ti,W)C-Based Cemented Carbonitrides*, Proc.PM$^2$tec. Vancouver, 1999.
[2] P. Ettmayer, H. Kolaska, W. Lengauer, K. Dreyer, *Int. J. Refr. Metals & Hard Mater*, **13** (1995) 343.
[3] A. Maurer, *J. Hard Mater*. **3** (1992) 235.
[4] K. Kokini, B. D. Choules, *Composite Eng.* **5** (1995) 865.
[5] C. Y. Jian, T. Hashida, H. Takahashi, M. Saito, *Composite Eng.* **5** (1995) 879.
[6] K. Hashimoto, P.-Y. Park, J.-H. Kim, H. Yoshioka, H. Mitzui, E. Akiyama, H. Hobazahi, A. Kawashi, K. Asami, *Mat. Sci. Eng. A* **196** (1995) 1.
[7] P. Cheang, K. A. Khor, *Biomaterials* **17** (1996) 537.
[8] J. R. Jacobson, *SPIE Procs.* **2046** (1995) 2.
[9] R.-Y. Tsai, C.-T. Wei, F. C. Ho, *SPIE Procs.* **2046** (1995) 189.
[10] F. C. Ho, C-H. Lee, R.-Y. Tsai, *SPIE Procs.* **2046** (1995) 197.
[11] S. Xue, W. Ousi-Benomar, A. Singh, Z. Wu, P. K. Kuo, *SPIE Procs.* **2046** (1995) 205.
[12] H. N. G. Wadley, L. M. Hsuing, R. L. Lankey, *Composite Eng.* **5** (1995) 935.
[13] R.L.Boxman, P. J. Martin, D. M. Sanders eds., *Handbook of Vacuum Arc Science and Technology*, Noyes Publications, Park Ridge, NJ (1995) 367.
[14] R.F. Bunshah (Ed.), *Handbook of Deposition Technologies for Films and Coatings*, Noyes Publications, parks Rige, NJ, 1994, 350 pp.
[15] H.R. Kaufman, *Adv. Electronics Electron Phys.* **36** (1974) 265.
[16] H.R. Kaufman, J.M.E. Harper, J.J. Cuomo, *J. Vac. Sci. Technol.* **21** (1982) 764.
[17] H.R. Kaufman, *J. Vac. Sci. Technol.* **21** (1982) 725.

[18] H.R. Kaufman, *J. Vac. Sci. Technol.* **A4** (1986) 764.
[19] N.F. Vershinin, B.B. Straumal, W. Gust, *J. Vac. Sci. Technol* **A14** (1996) 3252.
[20] N.F. Vershinin, V.G. Glebovsky, B.B. Straumal, W. Gust, H. Brongersma, *Appl. Surf. Sci.* **109/110** (1996) 437.
[21] B. Straumal, W. Gust, N.F. Vershinin, M. Friesel, M. Willander, *Surf. Coat. Technol.* **100/101** (1998) 316.
[22] N. Vershinin, R. Dimitriou, M. Benmaleck, B. Straumal, W. Gust, J. Vivas Hohl, *Surface & Coatings Technology* **125** (2000) 35.
[23] N. Vershinin, B. B. Straumal, W. Gust, *J. Vac. Sci. Technol.* **A 14** (1996) 3252.
[24] B. S. Danilin, V. K. Syrchin, Magnetron Sputtering Systems, Radio i Svjas' Publishers, Moscow (1982) (in Russian) pp. 41, 73.
[25] T. van Vorous, *Solid State Techn.* **19** (1976) 62.
[26] N. F. Vershinin, V. G. Glebovsky, B. B. Straumal, W. Gust, H. Brongersma, *Appl. Surf. Sci.*, **109/110** (1996) 437.